

## We develop a scalable workflow for parallel earthquake source inversion employing Bayesian methods.

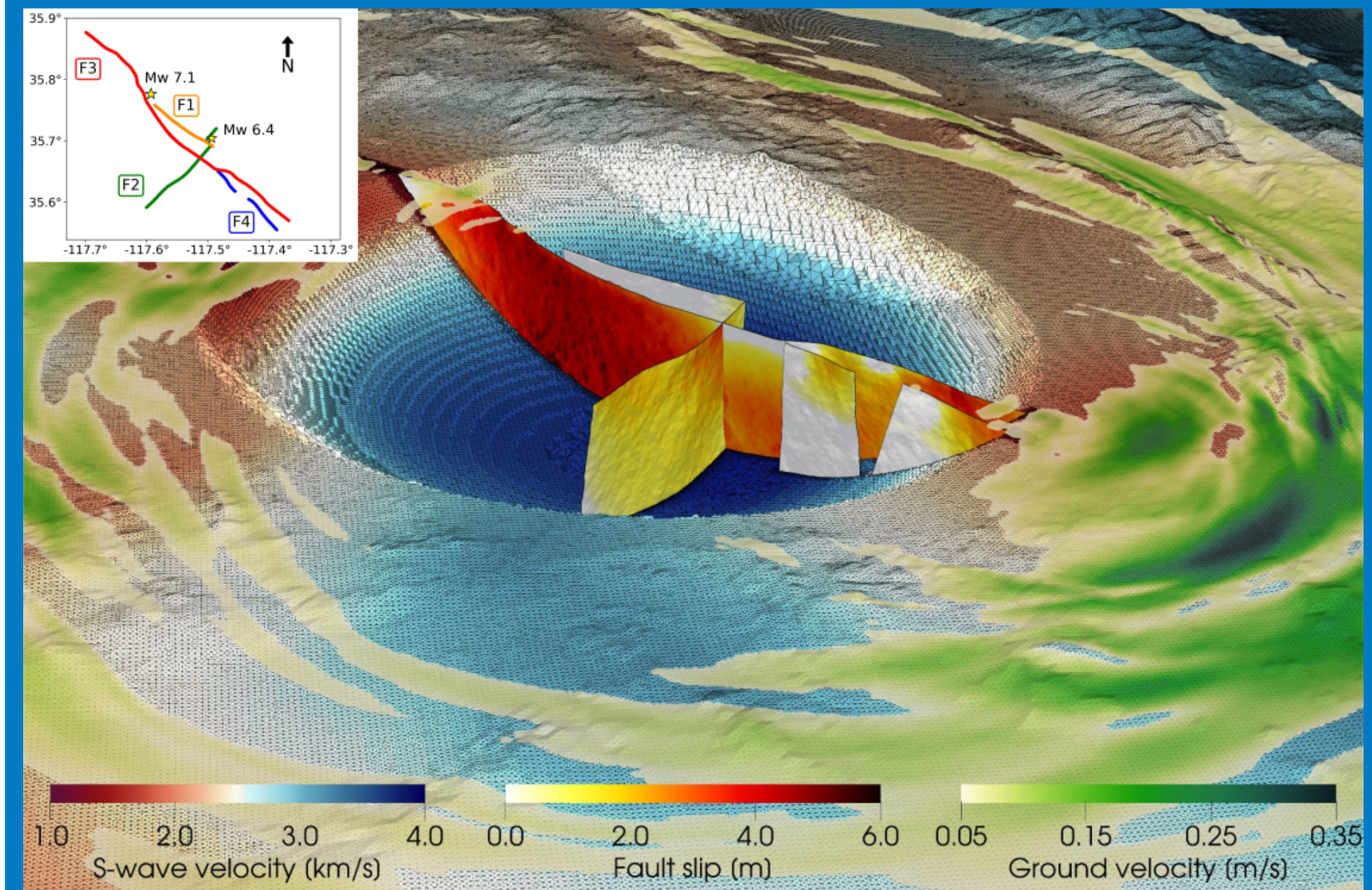


Figure 1: Ridgecrest scenario with complicated fault structure, topography and heterogeneous materials. Adapted from [3].

## Earthquake simulations with SeisSol

SeisSol (<https://seissol.org>) is a well-established simulation software for earthquakes source dynamics and seismic wave propagation. SeisSol solves the hyperbolic PDE

$$\partial_t q + A \partial_x q + B \partial_y q + C \partial_z q = Eq.$$

### Key features

**Realistic Materials** anisotropic elastic, isotropic elastic, poro-elastic and viscoelastic materials with optional plastic deformation

**Physics based sources** dynamic rupture, rate-and-state friction

**Geometric flexibility** with tetrahedral meshes

**Discontinuous Galerkin discretisation**

**High-order convergence** polynomial basis functions + ADER time-stepping

**Element local predictor corrector scheme** facilitates parallelization.

**Small matrix-matrix multiplications** code-generator YATeTo with architecture specific backend for node-level performance

**Parallelisation strategy**

**MPI + X** based on mesh partitioning

**OpenMP** for CPU clusters

**CUDA/SYCL** for GPU offloading

**Fused simulations**

**Compute  $N$  simulations simultaneously** by adding another dimension to the solution *tensor*.

**Reduce I/O overhead** Read mesh only once.

**No padding for SIMD** Choose number of simulations as a multiple of the vector register width.

**Reduce cache-transfers** element-local mass/stiffness matrices only loaded once per  $N$  simulations

**Scaling results**

**CoolMUC-2** 812 compute nodes, each with two Intel Xeon E5-2697 v3 processors and 64 GB RAM

**Improved strong scaling with fused simulations** due to higher computational workload per element

**Eight fused simulations optimal** 33% improvement over single simulations

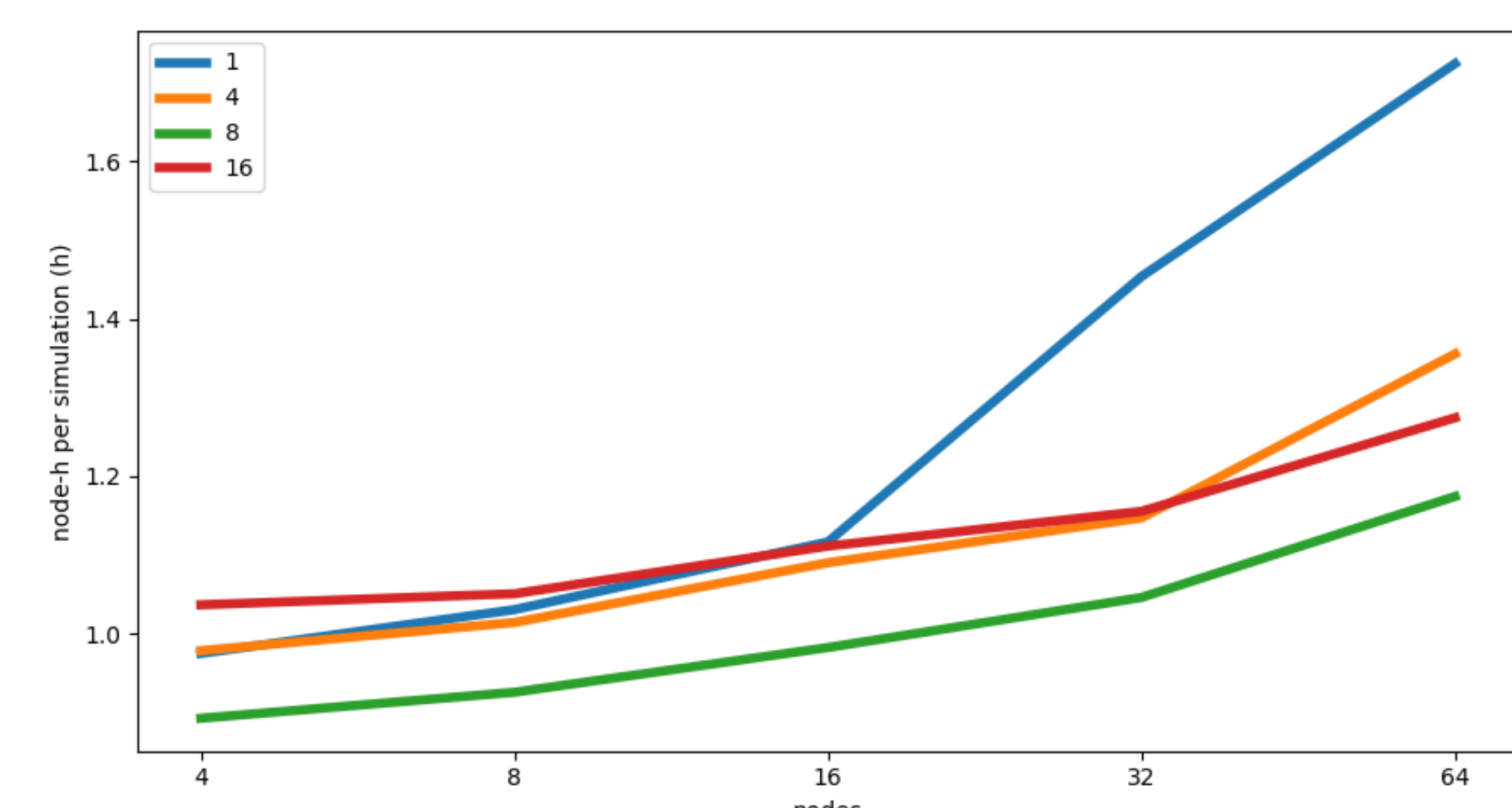


Figure 2: Computational effort per simulation for different number of fused simulations. The mesh contains 420000 elements. Using eight fused simulations, reduces the computational time by up to 33%.

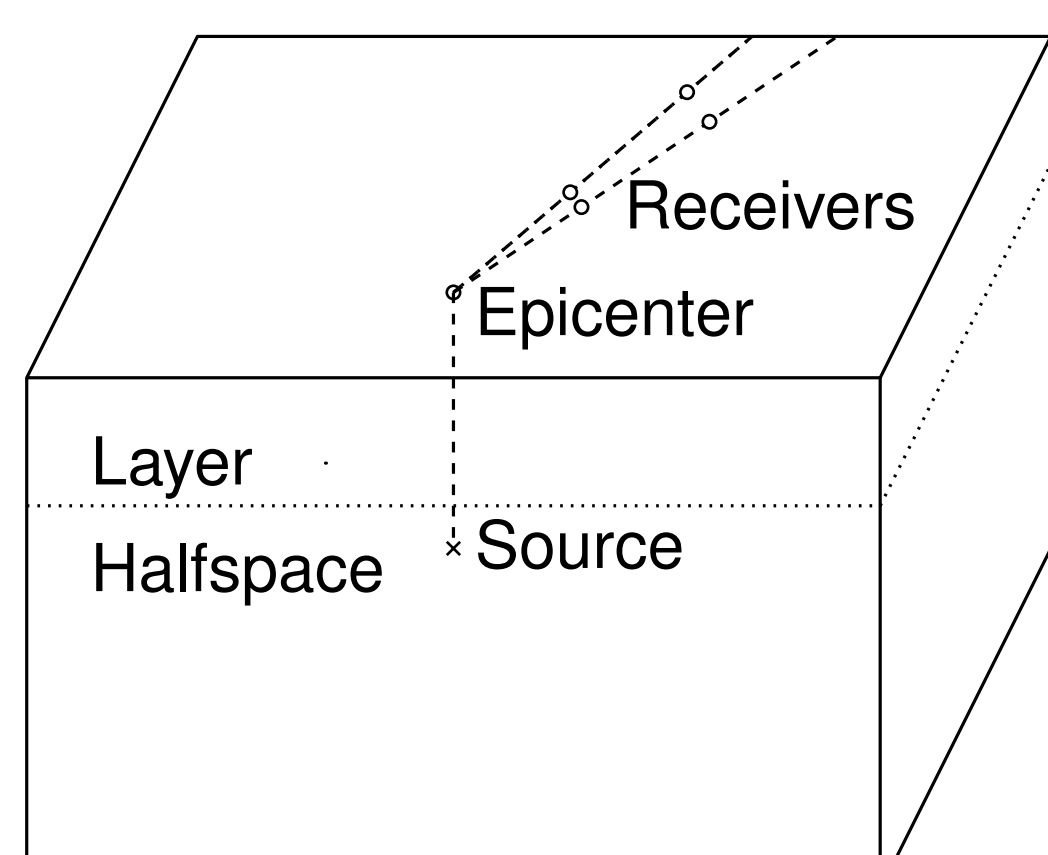


Figure 3: Geometry of the LOH1 scenario. The scenario features an elastic halfspace with a slow-velocity layer on top. A double couple source excites elastic waves, which are recorded at four surface receivers.

## Bayesian inverse problems with the Markov-Chain Monte-Carlo method

### MCMC sampling

Bayesian inverse problems allow us to solve inverse problems in a probabilistic manner, i.e. find the probability distribution of an unknown parameter  $\theta$ , which fits the data  $\hat{y}$ . Build a Markov chain of samples  $\theta_j$ :

**Draw new proposal**  $\theta'$  from proposal distribution  $q(\theta_j, \cdot)$ .

**Evaluate forward model**  $y' = G(\theta')$ .

**Compute proposal likelihood** by comparing  $y'$  with data  $\hat{y}$ .

**Accept/Reject** Accept  $\theta_{i+1} = \theta'$  with certain probability otherwise keep previous sample  $\theta_{i+1} = \theta_j$ .

**Stationary distribution**  $P(\theta|\hat{y}) \propto P(\hat{y}|\theta) \cdot \pi^0(\theta)$

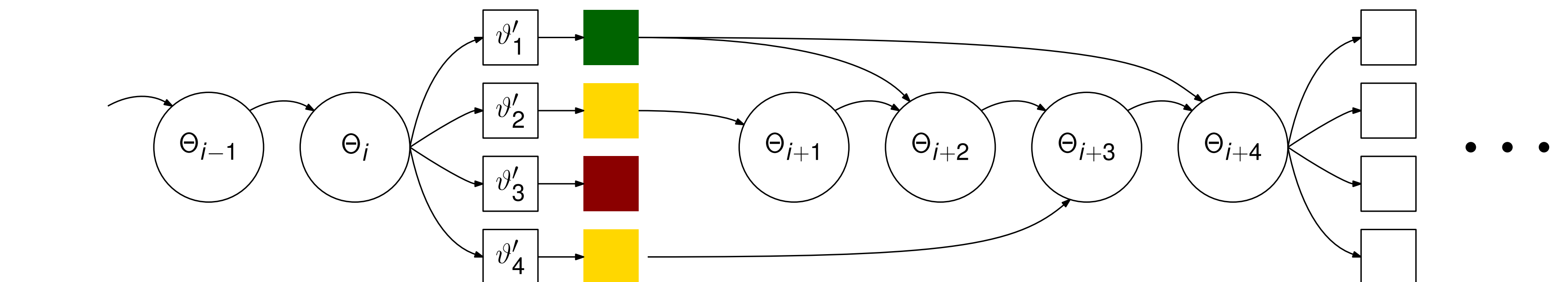


Figure 4: Sketch of the GMH algorithm for  $N = K = 4$ . Based on the sample  $\theta_i$ , four new proposals  $\theta'_j$  are drawn. The forward model is executed and in comparison to the data, a likelihood is assigned to each proposal (indicated by the colors). Based on this likelihood estimator, four new samples  $\theta_{i+1}, \dots, \theta_{i+4}$  are added to the Markov Chain.

## Performance of the Generalized Metropolis-Hastings algorithm

### Benchmarking GMH

We test the performance of the GMH algorithm on a simple ODE test case with two unknown model parameters.

**Vary  $N = 1, \dots, 20$ ,  $K = 1, \dots, N$**  to obtain 1000 samples.

**$K \ll N$  inefficient** high execution time, waste too many samples.

**Acceptance ratio increases with  $N$ .**

**$K \ll N$  generates more independent samples.**

**Use  $K = N$  with small  $N$**  for best ESS per time ratio.

Note that in this benchmark test, the speed-up of using fused simulations was not as high as it was for SeisSol.

### Performance metrics

**Acceptance Ratio** describes how many proposals are accepted as samples into the chain.

High acceptance ratio: exploration of the parameter space is insufficient. Low acceptance ratio: waste a lot of (expensive) samples.

**Effective sample size** subsequent samples of a Markov Chain are dependent, but we want to generate independent samples. The effective sample size (ESS) characterizes how many (approximately) independent samples have been drawn.

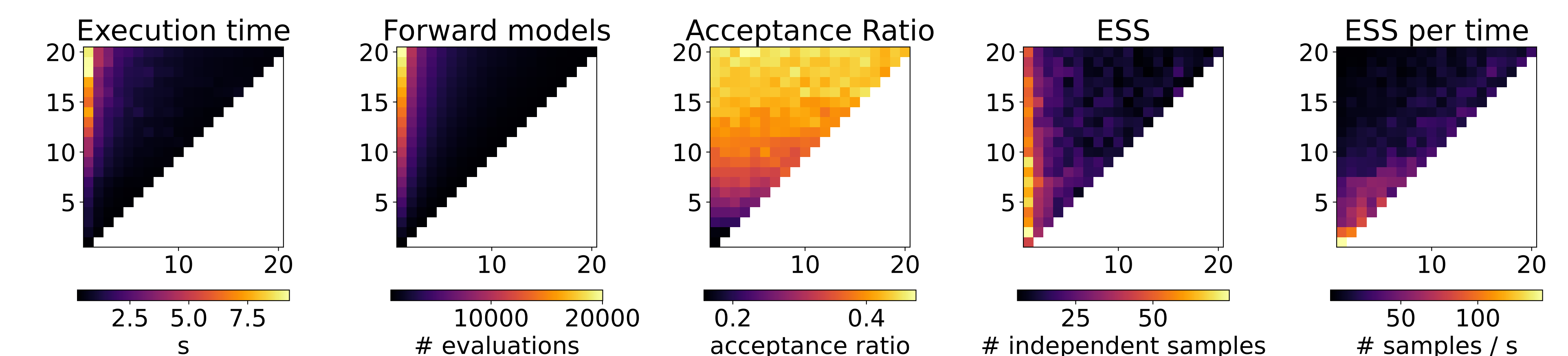


Figure 5: Performance metrics of the GMH algorithm for an ODE test case. The vertical axis denotes the number of fused simulations ( $N$ ) and the horizontal axis denotes the number of accepted samples ( $K$ ).

## Finding the source position of the LOH1 scenario with GMH sampling

### Model setup

**Unknown source position** c.f. fig. 3

**Ground truth**  $\hat{\theta} = (0, 0, 2000)^T$

**Data  $\hat{y}$**  semianalytic solution of receiver seismograms

### Implementation

**Use SeisSol** with fused simulation,  $N = 8$ .

**Fused GMH kernel** patch of MUQ library [2].

**Compare result with data  $\hat{y}$**  using  $\|\cdot\|_1$  norm.

**Runtime 21 h** on 32 nodes to collect 640 samples

### Results

**$\mathbb{E}(\theta)$  slightly off** with significant offset in  $x/y$  direction:  $(-471.4, 733.7, 2232)^T$

**Receiver 2 and 4 match well.**

**Receiver 1 and 3 are troubled** in particular  $v_3$ .

**Acceptance ratio = 11 %**, **ESS = 8**

### Upcoming work

**Improve acceptance ratio and ESS.**

**More unknowns** e.g. source orientation, frequency

**Realistic scenario** dynamic rupture, topography

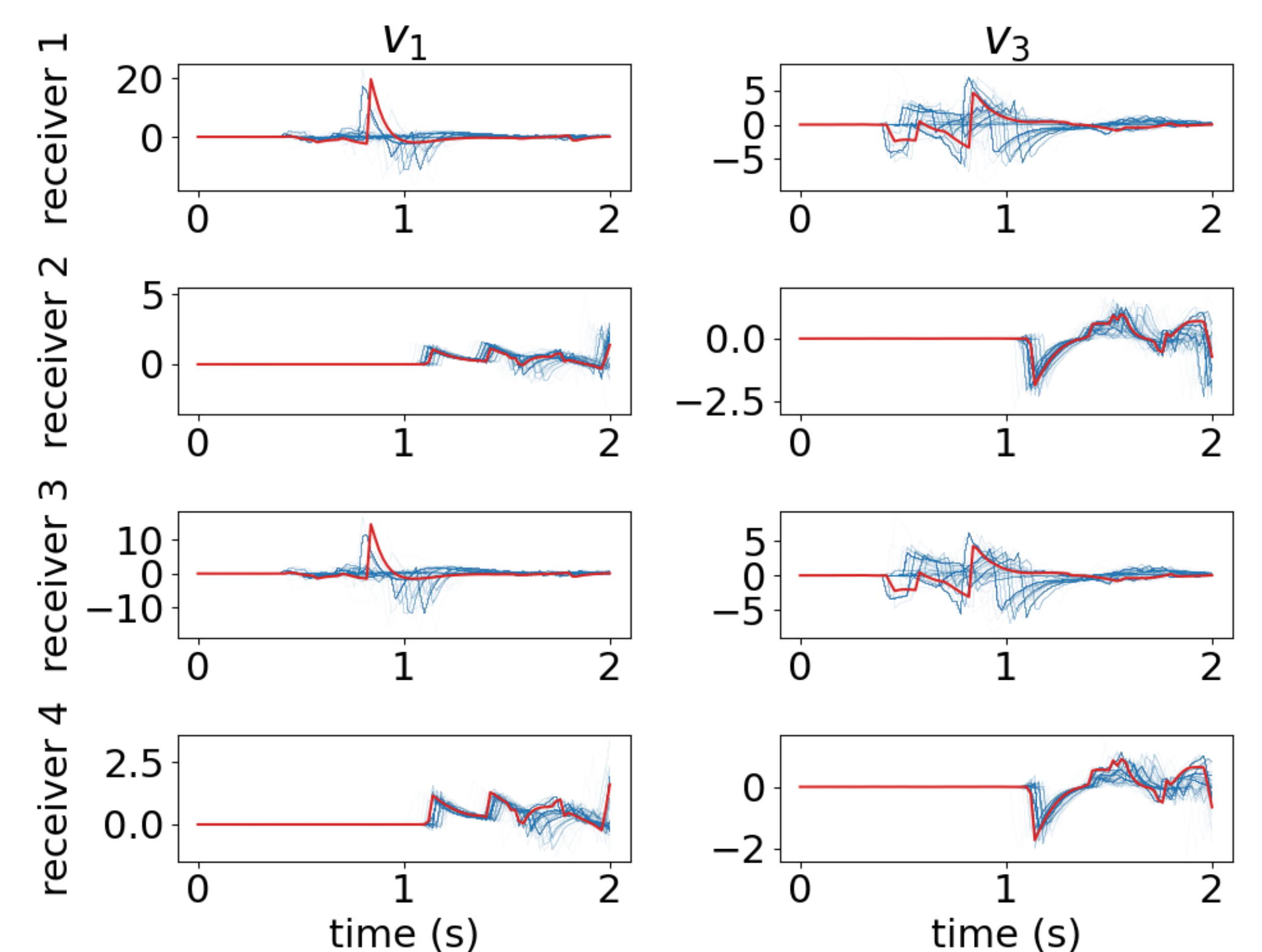


Figure 6: Comparison of the reference solution (red) and the MCMC samples (blue).

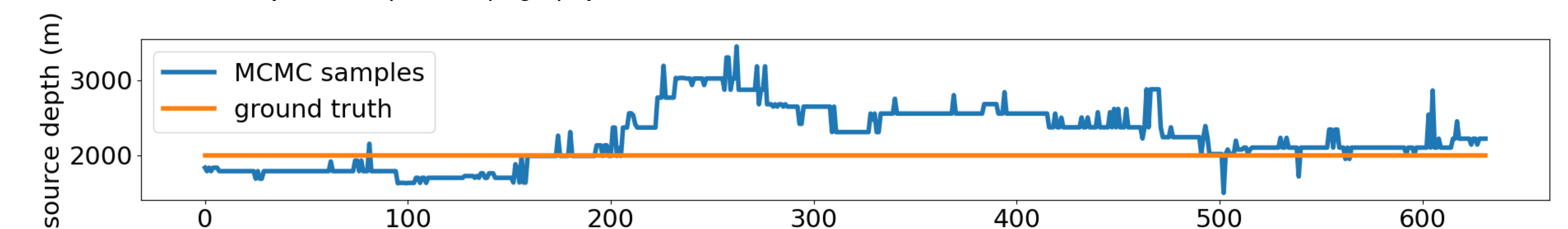
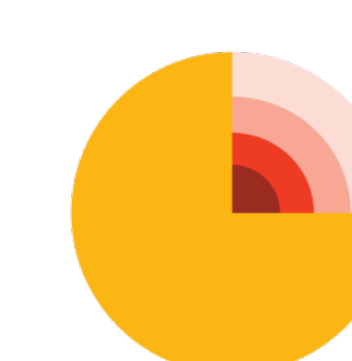


Figure 7: Source depth samples gathered during the MCMC inversion of the LOH1 example.

## References

- [1] B. Calderhead. "A general construction for parallelizing Metropolis-Hastings algorithms". In: *Proceedings of the National Academy of Sciences* 111.49 (Dec. 2014). Publisher: Proceedings of the National Academy of Sciences, pp. 17408–17413. DOI: 10.1073/pnas.1408184111.
- [2] M. Parno et al. *MIT uncertainty quantification (MUQ) library*. 2014.
- [3] N. Schliwa, A.-A. Gabriel, and Y. Ben-Zion. "3D Modeling of near-field ground motions and deformation in dynamic rupture simulations of the 2019 Ridgecrest earthquake including fault zone and fault roughness effects". Poster Presentation. 2023 SCEC Annual Meeting (Palm Springs, CA), Sept. 10, 2023.

## Acknowledgement



The research leading to these results has received funding from Horizon Europe (ChEES-2P grant No. 101093038).

## Github

